Journal of Non-Crystalline Solids 605 (2023) 122174

Contents lists available at ScienceDirect

Journal of Non-Crystalline Solids

journal homepage: www.elsevier.com/locate/jnoncrysol

Improving the precision of Vickers indentation measurements in soda-lime glass with increased dwell time

W. Porter Weeks [a], Katharine M. Flores [a,b,*]

[a] Institute of Materials Science and Engineering, Washington University in St. Louis, United States
[b] Department of Mechanical Engineering and Materials Science, Washington University in St. Louis, United States

ARTICLE INFO

Keywords:
Vickers indentation
Indentation fracture toughness
Silicate glass

ABSTRACT

Vickers indentation methods are popular techniques for the determination of hardness, indentation fracture toughness, and crack initiation resistance in silicate glasses, predominantly due to the simplicity and efficiency of the technique. Despite the method's popularity, it is challenging to obtain consistent and repeatable results from these measurements. Here, we perform a systematic investigation of the effects of applied load, dwell time, and post-indentation observation time on the precision of hardness and indentation fracture toughness values for soda-lime silicate glass measured via Vickers microindentation. The data suggests that low applied loads ($\leq$ 1.06 N) in combination with short dwell times ($\leq$ 15 s) lead to low precision in the measurements and that a longer dwell time of 30 s leads to higher precision and load-independent indentation fracture toughness. The increased repeatability of these measurements at higher dwell time could make Vickers microindentation a reliable technique for silicate glass mechanical property measurement.

1. Introduction

Vickers indentation is an extremely common method for the determination of hardness [1–19], indentation fracture toughness [3–10,17–19], and crack initiation resistance [1,20–38] in silicate glasses. While the simplicity of the Vickers method has driven its popularity, historically there has been a lack of repeatability, particularly in the determination of hardness (H_v) and indentation fracture toughness (K_c). To illustrate this problem, optimized models to predict H_v [1–8,10,12–14,17–19], and density [2–8,12,17,39–46] based on compositional and structural terms were compared with reported results for various silicate glass compositions, as described in the Supplementary Information (Fig. S1). While these datasets are not comprehensive, the poor agreement between the modeled and observed values for H_v and K_c (R^2 = 0.801 and 0.826, respectively) illustrates the aforementioned lack of precision in these measurements in contrast to the excellent fit associated with the model of density (R^2 = 0.9908), a historically repeatable measurement.

In the present work, we wish to understand why there is such poor consistency in Vickers indentation measurements for silicates. Beyond the glass composition itself, several factors of interest could contribute to the variability in the measured values, including variations in environmental conditions during testing (e.g. temperature and humidity) [25,47–51], densification during indentation [2,7,12,21,28,52,53], indenter tip geometry [54], and the experimental conditions of the measurement (applied load and dwell time). The effect of applied load on Vickers indentation measurements has been heavily investigated, as the study of crack initiation resistance intrinsically involves varying the applied loads to determine the load at which cracking occurs in a given composition [1,20–35,37,38,52]. The literature is much sparser for the effect of dwell time during Vickers indentation. While studies have investigated the effect of dwell time on measured hardness [55–57], only one of these was performed on silicate glass [57], focusing on the difference in behavior as a function of the surrounding environment. The effect of dwell time on nanoindentation measurements has also been investigated in a variety of materials [58,59]. In addition, Lawn et al. investigated the combined effects of applied load and dwell time on crack initiation in soda-lime glasses [60], although this study focused on the kinetics of shear transformations. Despite the general lack of systematic dwell time investigations, an extensive review of the literature [1–38] shows that 10–15 s is the overwhelming dwell time of choice (Fig. 1). Only one study was found with a dwell time of more than 15 s [5] and another failed to report any dwell time at all [3].

* Corresponding author at: Institute of Materials Science and Engineering, Washington University in St. Louis, United States.
E-mail address: floresk@wustl.edu (K.M. Flores).

https://doi.org/10.1016/j.jnoncrysol.2023.122174
Received 26 September 2022; Received in revised form 24 January 2023; Accepted 26 January 2023
Available online 4 February 2023

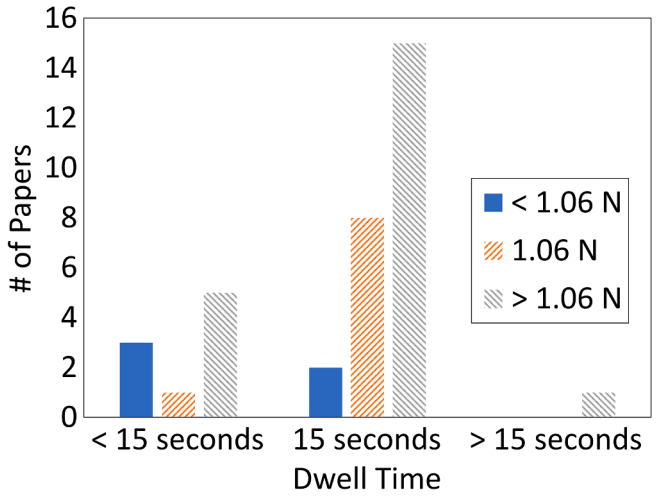

Fig. 1. Distribution of reported applied loads and dwell times from previous Vickers indentation studies of silicate glasses [1,2,4–38].

While the ASTM E384 standard for Vickers hardness measurements suggests a dwell time of 10–15 s [61], we were unable to find any justification in the literature for this recommendation. This is echoed by Bechgaard et al., who stated that "no reason is given for the choice of dwell time in any of the 32 papers" that they investigated [25]. If there is no reason for the choice, then one should ask if there is any reason to believe that the selection of dwell time will significantly affect the measured H_v and K_c of silicate glasses. In a 1987 study, Hirao and Tomozawa observed a significant decrease in the measured Knoop hardness in an air environment as a function of dwell time under various applied loads [57]. In addition, an indentation size effect has long been known to occur in fused silica [62] and silicate glasses [63,64] where the hardness has been shown to decrease as a function of the applied load. While the origin of this indentation size effect is still debated in the literature [65–67], it has also been observed for H_v of single crystals and ceramics [68,69] suggesting that a similar phenomenon may be observed in H_v of silicate glasses. In addition, Lawn et al. [60] showed that sufficient dwell time is required for consistent crack pop-ins in silicate glasses, in that short dwell times led to inconsistency in cracking patterns, and that the dwell time required for consistent cracking decreases as applied load is increased. While Lawn et al. [60] did not specifically address determination of H_v or K_c, the reported correlation between dwell time and cracking patterns suggests that one should consider the effect that short dwell times have on Vickers indentation measurements, particularly when combined with low applied loads.

Dwell time studies of polymers [55] and composites [56] both lead to the conclusion that the combination of short dwell time and low applied load yields a lack of statistical precision in measured indentation results with one claiming that "the results of this study showed that lower ranges of indentation load and dwell time used in the literature may not be acceptable for some materials" [56]. We argue that the aforementioned studies [55–57,60] provide ample reason to hypothesize that the variation of dwell time will have a significant effect on Vickers indentation measurements in silicates. This leads to the current study investigating how applied load and dwell time affect the values and precision of H_v and K_c. The primary goal is to determine if changing either of these experimental parameters could lead to higher consistency in Vickers indentation measurements than is currently observed in the literature. If so, this could drastically improve the practicality of this method for the evaluation of silicate glass mechanical properties.

2. Experimental methods

2.1. Vickers microindentation measurements

Vickers microindentation measurements were performed for the combinations of applied loads and dwell times provided in Table 1. While we were able to obtain 25 replicates for most of the conditions, the combination of the lowest load and dwell time (0.27 N, 15 s) proved challenging, such that only 20 usable replicates of the condition were produced. The indentations were performed on soda-lime glass slides (Fisherbrand Microscope slides; 25 mm × 75 mm × 1 mm) with a Vickers diamond tip on a Leitz Microindenter (Model 000–366–902). Birefringence measurements confirmed that the residual stresses in the slides were negligible. The replicates for a given condition were performed on a single glass slide, with the indents spaced such that no two indents were closer together than 7 mm (10 indents along the 75 mm length; 3 rows along 25 mm width). Each indent was imaged on a Nikon optical microscope (Nikon Eclipse LV150N) at seven time points after indentation, with the first image taken between 60 s and 1900s after the indenter was removed and the last image taken approximately one week after indentation, yielding 7 images per replicate and a total of 1365 images. The indent size and crack lengths were measured using the image analysis software ImageJ for every image of each indent [70]. Utilizing the length measurement tool in ImageJ, the indent size was determined by averaging the two diagonal lengths of the indent, and the crack length was determined by averaging the length of all four cracks (each measured from the center of the indent to the tip of the crack). The temperature and humidity in the laboratory were monitored and recorded over the entire 7-day duration of the experiment (see Supplementary Fig. S2).

Vickers hardness (H_v) in units of GPa was calculated using Eq. (1), where F and L are the applied load and diagonal length of the indent in units of Newtons and micrometers, respectively:

$$H_v = 18.19\frac{F}{L^2} \tag{1}$$

Indentation fracture toughness (K_c) in units of MPa$\sqrt{\text{m}}$ was calculated using the approach of Anstis et al. [71], as shown in Eq. (2), where F and c are the applied load and crack length from the center of the indent in units of Newtons and micrometers, respectively:

$$K_c = 0.156\frac{F(E/H_v)^{0.5}}{c^{1.5}} \tag{2}$$

Here, E is the elastic modulus of the material (assumed to be 72 GPa for soda-lime glass) [72] and H_v is the hardness calculated by Eq. (1). Because K_c is calculated from the length of a single crack, the reported value for a given indent is the average of the K_c calculated from the four cracks emanating from the four corners of the indent. While Niihara et al. have proposed alternate calculations for the indentation fracture toughness [73], these equations were originally designed for Palmqvist cracks. In the present work, the length of the cracks relative to the size of the indent suggests that we have half-penny cracks, which are more appropriately described by Eq. (2).

Table 1
Applied loads and dwell times investigated in this study.

Applied Load (N)	Dwell Time (s)	Replicates
0.27	15	20
0.45	15	25
1.06	15	25
1.91	15	25
0.27	30	25
0.45	30	25
1.06	30	25
1.91	30	25

2.2. Statistical analysis

Much of the discussion in this paper focuses on the statistical significance of differences in the data sets measured using various combinations of testing conditions. In order to perform these analyses, data sets were first subjected to an F-test to determine whether the variances of the data sets are similar enough to be considered equal. Based on these results, the data sets were then subjected to a *t*-test for statistical significance for either unequal or equal variances, as appropriate. Finally, the statistical significance of the differences between the data sets was quantified by the two-tail p-value of the *t*-test. We define p-values ≤ 0.05 to indicate statistically significant differences in the data.

3. Results

3.1. Indent size and Vickers hardness

The indent size as a function of applied load and dwell time are shown in Fig. 2a, with two-tail p-values provided to compare the results for 15 s and 30 s dwell times at each load. As expected, the average size of the indent (from the replicates of each condition) increased as the applied load increased. The average indent size depended on dwell time at all loading conditions except for 1.06 N. Moreover, the standard deviation of the indent sizes across the 20–25 replicates created at a given load (denoted by the error bars) decreased significantly at the higher dwell time, with a p-value of 0.0288 between the standard deviations at 15 s and 30 s.

Due to the dependence of hardness on indent size, these trends extend to H_v, calculated from Eq. (1), as shown in Fig. 2b. In addition, at higher applied loads the value of H_v approaches values reported in the literature [5] shown by the red band, which were obtained at loads of up to 9.81 N. The hardness is significantly over-estimated (up to four times larger than reported values) in the low-load conditions.

3.2. Crack length and indentation fracture toughness

Not all indents yielded an appropriate indentation crack pattern necessary for accurate measurement of crack length and K_c, with some indents created at the lowest loads exhibiting no cracks, and others exhibiting irregular crack patterns. A "measurable crack pattern" was defined as an indent with four straight cracks of approximately the same length radiating from the corners of the indent with minimal additional cracking. Supplementary Fig. S3 provides example images of indents with no cracks, irregular cracks, and cracks suitable for K_c determination. (Note that all three examples in this figure were created using the same load and dwell time conditions, illustrating the need for multiple replicates to obtain reliable data.)

Fig. 3 shows the fraction of indents that formed measurable crack patterns for all investigated conditions. None of the 0.27 N indents produced a measurable crack pattern; this load will not be considered with regards to crack length and indentation fracture toughness measurements. The measurable fraction was also very low (< 40%) for the 0.45 N indents. Thus, most of the analysis below focuses on the 1.06 N and 1.91 N conditions. The measurable fraction tended to increase logarithmically with time after indentation, as cracks initiate due to the residual stress around the indent. The measureable fraction also increased with dwell time for the 1.06 N loading condition, but decreased with dwell time for the 0.45 N loading condition. However, nearly all samples immediately formed measurable cracks at 1.91 N at both dwell times.

The length of the measurable cracks formed for the 15 s and 30 s dwell times are compared in Fig. 4a as a function of time after indentation. Higher applied loads produced longer cracks, as may be expected. The error in the crack length is extremely high for the 1.06 N, 15 s dwell time condition. The data exhibited a significantly lower standard deviation at this applied load when the dwell time was raised to 30 s (p-value of 1.17×10^{-11}, comparing standard deviations). Somewhat surprisingly, the 30 s condition also exhibited a significantly lower average

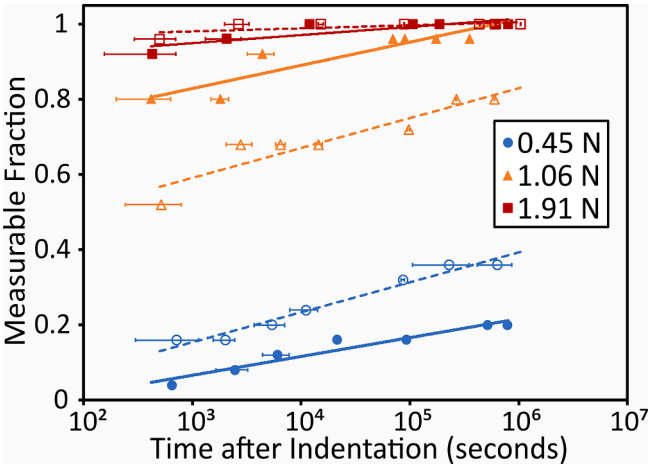

Fig. 3. Fraction of indents that formed measurable crack patterns as a function of applied load and time after indentation for 15 s (open symbols/dashed lines) and 30 s (closed symbols/solid lines) dwell time conditions.

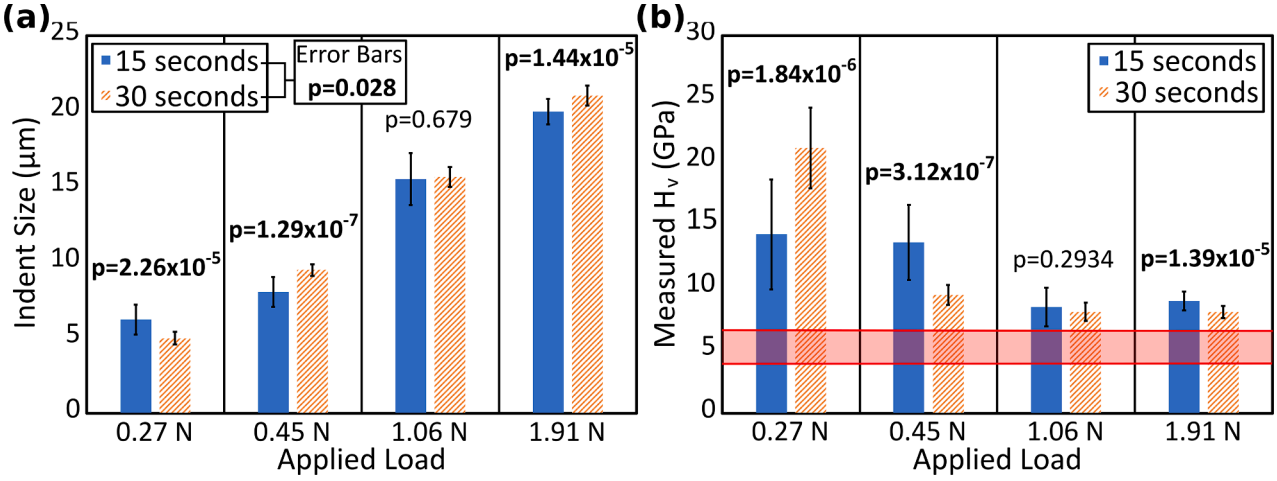

Fig. 2. (a) Indent size and (b) Vickers hardness as a function of applied load and dwell time, where the red band represents hardness values reported in the literature for soda-lime glass [5]. Measured values are averaged over replicates of each condition and the error bars represent the standard deviation between these replicates.

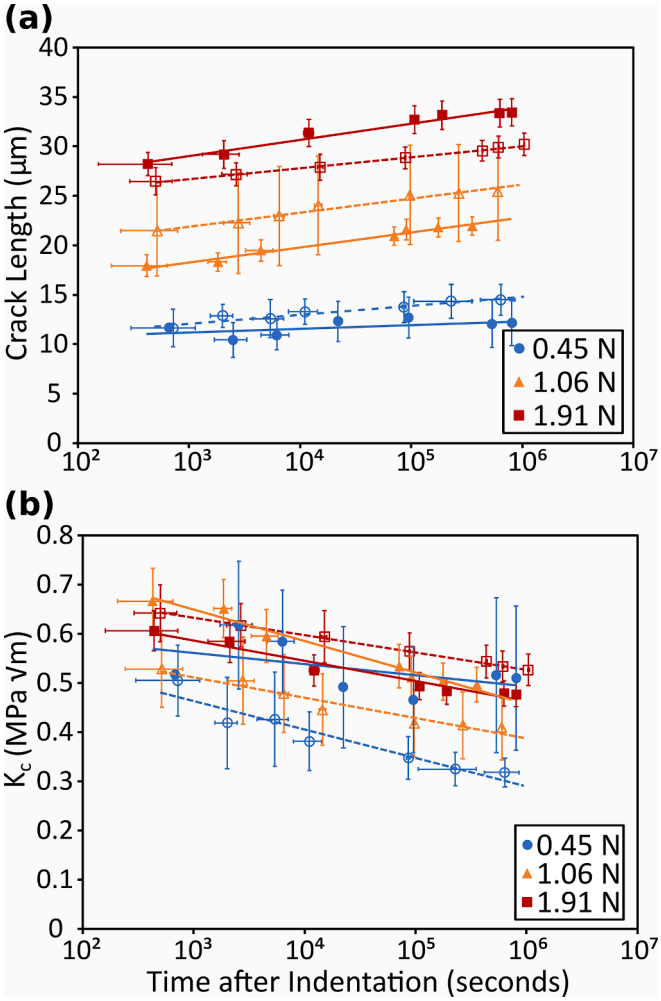

Fig. 4. (a): Crack length as a function of time after indentation for 15 s and 30 s dwell times at each load; (b): Indentation fracture toughness as a function of time after indentation for 15 s and 30 s dwell times at each load. 15 s dwell time data are shown as open symbols with dashed lines and 30 s dwell time data are shown as filled symbols with solid lines.

crack length than the 15 s dwell time condition at this load (p-value of 0.00213).

The indentation fracture toughness was calculated for each indent with a measurable crack pattern using Eqs. (1) and (2) and is plotted in Fig. 4b again as a function of time after indentation. The indentation fracture toughness was dependent upon the applied load when a 15 s dwell time was utilized whereas the data collapsed into a single band for all loads at the higher dwell time of 30 s. Moreover, there was a statistically significant difference between the 15 s and 30 s dwell time conditions at applied loads of 0.45 N and 1.06 N while the 1.91 N loading showed no significant variation in K_c as a function of dwell time (see p-value comparison in Table 2).

4. Discussion

In the present work, we measured the indent size and crack lengths for each indent at 7 time intervals after indentation. Although the crack length may increase with time as the system relaxes (Fig. 4a), the size of the indent remains constant over the duration of the 7 observations (Supplementary Fig. S4), and thus we can describe the size of each indent and the corresponding hardness by the average of the 7 values. Variation among these 7 values is the result of inconsistencies in the indent size observation itself: how the sample is placed on the microscope, how the microscope is focused, etc. Below, we use this variation to quantify the "observation error" for our data through an error propagation analysis. Furthermore, we repeated our indentation experiments 20–25 times for each combination of applied load and dwell time, producing a set of 20–25 data points (each averaging over 7 observations) for each condition. The variation in this dataset represents the statistical distribution of the measurements across multiple experiments, which we describe below as the "total error".

Table 2
Tabulated p-values comparing the indentation fracture toughness data obtained at each combination of applied load and dwell time, where the p-values ≤ 0.05 are deemed significant (bolded). Each p-value compares the conditions denoted by the corresponding row and column headings.

Indentation Fracture Toughness	1.06 N, 15 s	1.91 N, 15 s	0.45 N, 30 s	1.06 N, 30 s	1.91 N, 30 s
0.45 N, 15 s	**0.04809**	**5.03×10^{-5}**	**0.0011**	**5.91×10^{-4}**	**0.00171**
1.06 N, 15 s	–	**0.00045**	**0.0244**	**0.0087**	**0.0416**
1.91 N, 15 s		–	0.0937	0.732	0.0565
0.45 N, 30 s			–	0.305	0.792
1.06 N, 30 s				–	0.217

4.1. Determination of observation error

To determine the most appropriate indentation load and dwell times to identify meaningful variations in properties across a set of material compositions or processing conditions being compared, we must consider how to separate variations due to physical (structural) differences in the materials themselves from scatter that can be attributed to the repeatability of the observation process, i.e. placing the sample on the microscope stage, focusing the microscope, and measuring the size of a given indent. We define the latter variability as the "observation error", and primarily consider its impact on the observation of indent size and crack length. Here, we calculate the observation error using the principles of error propagation, a common statistical technique in the calculation of compounded errors in measured quantities [74].

First, we note that the size of a particular indent does not change as a function of time after indentation (Supplementary Fig. S4) due to the extremely limited kinetic ability of the atoms within the glass to change their configuration at room temperature without an externally applied force. Therefore, any variation in the indent size measured from all images of a particular indent is assumed to be a consequence of error in the observation method as opposed to physical changes within the material. We can determine ΔH_v, the compounded error in the calculated H_v, by differentiating Eq. (1) with respect to indent size (L), multiplying by the observation error in the indent size, ΔL, and taking the absolute value of the result:

$$\Delta H_v = \left|\frac{dH_v}{dL}\Delta L\right| = \left|\frac{-36.38F}{L_{ave}^3}\Delta L\right| \quad (3)$$

In Eq. (3), L_{ave} is the average indent size across the 20–25 replicates for a given condition. We determine the observation error ΔL by calculating the standard deviation of the 7 indent size measurements for each replicate of a condition and then taking the average of these standard deviations across all 20–25 replicates. The result of Eq. (3) yields the portion of the standard deviation in H_v for a given set of loading and dwell time conditions that is attributable to observation error.

Using similar logic, we can determine the compounded observation error for K_c. Unlike the assumption about indent size, the crack lengths may not remain constant as a function of time after the indent. Furthermore, we cannot assume that all of the cracks within a given image will be exactly the same length. Therefore, we will assume that the observation error in the crack length, Δc, is the same as the observation error in the indent size, ΔL, since any observation error associated with our ability to consistently measure the indent size would likely

propagate to the crack length values obtained using the same method. Notably, this is a lower estimation on Δc, as crack lengths are more difficult to measure than indent sizes. To calculate the compounded error in K_c, we first substitute Eq. (1) into Eq. (2) to obtain a simplified expression for K_c in terms of L and c:

$$K_c = 0.0365\frac{(FE)^{0.5}L}{c^{1.5}}$$

We differentiate this expression with respect to L and c, multiply both derivatives by the corresponding observation errors, and sum the results to obtain the compounded error of the indentation fracture toughness, ΔK_c:

$$\begin{aligned}\Delta K_c &= \left|\frac{\partial K_c}{\partial L}\Delta L\right| + \left|\frac{\partial K_c}{\partial c}\Delta c\right| \\ &= \left|\frac{0.0365\ (FE)^{0.5}}{c_{ave}^{1.5}}\Delta L\right| + \left|\frac{-(1.5)(0.0365)(FE)^{0.5}L_{ave}}{c_{ave}^{2.5}}\Delta L\right| \end{aligned} \quad (4)$$

Where c_{ave} is the average crack length across the replicates of a condition and we have used the assumption that $\Delta c = \Delta L$. From Eqs. (3) and (4), we can calculate the variation in the Vickers hardness and indentation fracture toughness measurements that are consequences of the observation error as opposed to physical differences across the samples, such as initial defect density, as described below.

4.2. Indent size and Vickers hardness

Fig. 2 shows that there is a statistically significant effect of dwell time on indent size and H_v at all but one of the applied loads (1.06 N). While the increase in indent size at 0.45 N and 1.91 N with increased dwell time makes intuitive sense in the context of densification, the reason for the *decrease* in indent size as a function of dwell time at an applied load of 0.27 N is unclear. We also observe that the standard deviation of the indent size decreases significantly for the longer dwell time, suggesting that increasing the dwell time affects both the average indent size and the precision of the measurements. Fig. 5 provides additional insight into this relationship between dwell time and precision. Fig. 5a and b compare the observation error in indent size and H_v, obtained by analyzing the propagation of error, to the standard deviation in the measured values (averaged over the 7 observations for each indent) across all 20–25 replicates for a given condition. We define this standard deviation as the "total" error; this corresponds to the error bars in Fig. 2.

The total error and observation error are explicitly defined as the standard deviation measured across all replicates of a condition and the propagated error attributable to the observation techniques, respectively. The "residual error" (total error – observation error) for each condition are shown in Fig. 5c and d. A residual error less than or equal to zero indicates that any differences between the measured values are attributable to observation error, whereas a large positive residual error indicates that there are additional variations in the measured values which cannot be attributed to our limited ability to repeatably measure the indent size. For otherwise identical materials, these additional differences may be associated with incomplete densification of the local glass network and/or the development of non-uniform stress fields. In the case of both indent size and H_v, one observes large residual errors for

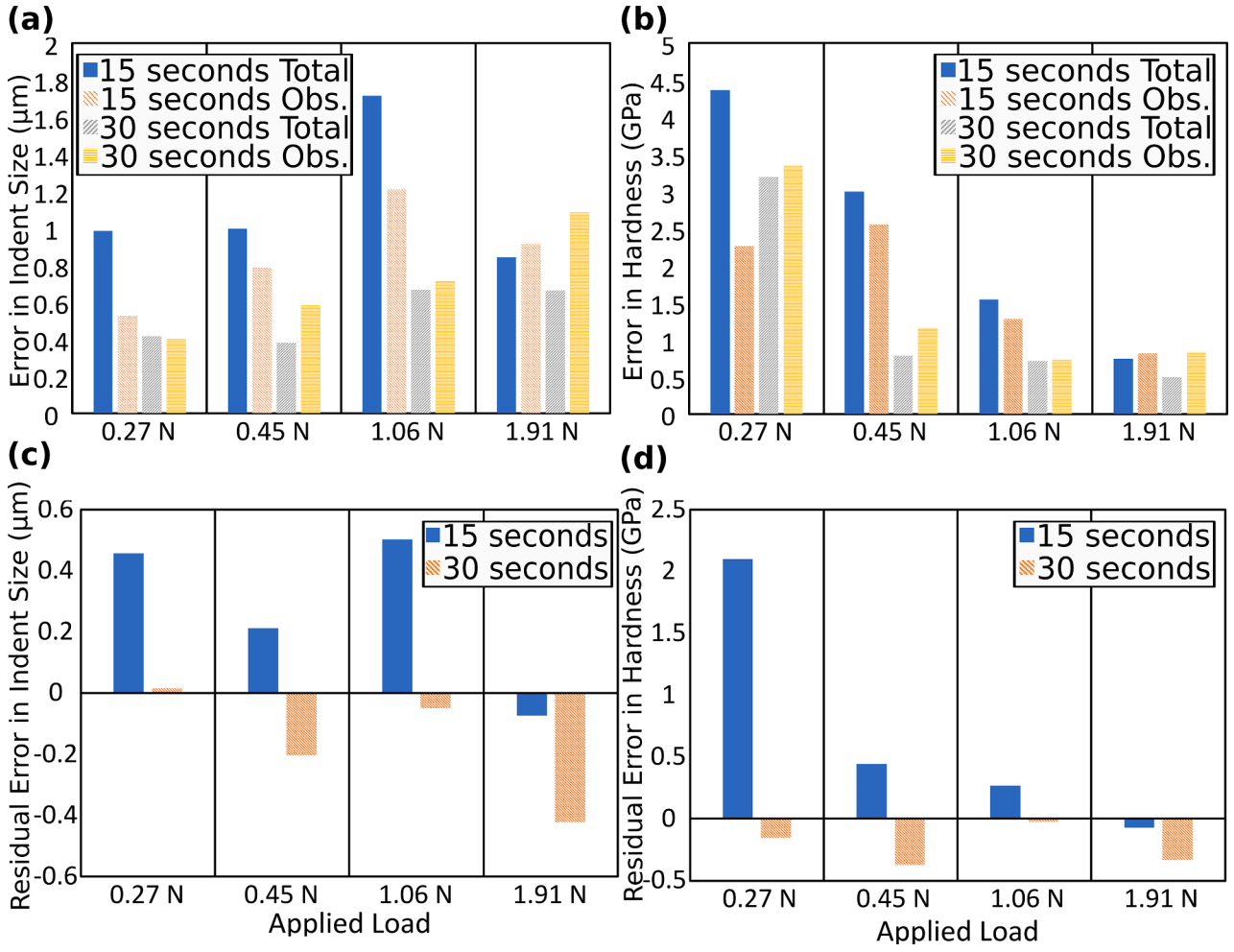

Fig. 5. (a-b): Total and observation errors for (a) indent size and (b) hardness. (c-d): Residual error (total – observed) for (c) indent size and (d) hardness.

the 15 s dwell time at all but the highest applied load, and negative residual errors for experiments conducted with 30 s dwell time regardless of applied load. This analysis is consistent with the statistically significant decrease in total error as a function of dwell time observed in Fig. 2. The 30 s dwell time increases the precision of these measurements, eliminating the residual error.

Cumulative probability plots of the indent size are presented in Fig. 6 for the 15 s and 30 s dwell time conditions. These plots are created with the "probplot" function in MATLAB, which calculates the z-score of each indent size, which is given by the difference between the point value and mean of the dataset, divided by the standard deviation of the dataset. Assuming a normal distribution, the function determines the cumulative probability as the fraction of data points within the dataset that have a z-score less than that of a given indent. In Fig. 6, dashed lines correspond to 95% confidence intervals for the 7 measurements made for a given indent, and solid lines indicate 95% confidence intervals for the set of 25 replicates for each condition. The dotted lines represent the normal distribution fits to each data set, calculated using the corresponding mean and standard deviation values. (Note that the vertical axis is scaled such that the normal distribution fit produces a straight line.)

For the 15 s dwell time (Fig. 6a), the 1.91 N loading condition is the only one where the normal distribution falls well within the 95% confidence intervals over the full range of the data, while the distributions of indent sizes at lower loads are less effectively characterized by a normal distribution. Therefore, not only is there residual error in these low load-short dwell time conditions (Fig. 5c), but this error is non-random in nature because it cannot effectively be fit by a normal distribution. This data suggests that there is a systematic bias affecting the 15 s dwell time conditions except at the highest applied load. Increasing the dwell time to 30 s (Fig. 6b) yields better fits to normal distributions, as well as better precision (higher slope, indicating a smaller standard deviation as seen in Fig. 5a). This improved fit to the normal distribution suggests that the systematic bias present at 15 s is not observed for the longer dwell time and shows that 25 data points are sufficient for normal distribution fitting in the case of indent size. While the exact cause of the systematic error for the 15 s dwell time remains unknown, we note that the normal distribution over-predicts the probability at larger indent sizes (i.e. the experimental probability of forming large indents is lower than expected), which suggests that 15 s may be insufficient time for complete densification to occur under the indents. The better fits for the 30 s dwell time are consistent with this hypothesis; 30 s is likely sufficient for complete densification to occur, reducing the systematic error. These results suggest that using higher applied loads and/or longer dwell time increases the precision of the measured indent size and, in turn, H_v.

4.3. Crack length and indentation fracture toughness

Fig. 4 clearly illustrates that the choice of indentation load impacts the measured indentation fracture toughness, with statistically significant lower indentation fracture toughness values observed for lower indentation loads as well as shorter dwell times, as denoted by the p-values in Table 2. The indentation fracture toughness values become statistically indistinguishable when either the highest applied load (1.91 N) or the longest dwell time (30 s) is utilized.

We again ask how much of the scatter in the values obtained under different combinations of load and dwell time can be attributed to observation error. The contribution of observation error to the calculation of K_c for each condition is determined using Eq. (4) and compared with the total error in Fig. 7, along with the errors in the crack length. We first note that the residual error in the crack length measurement (measured relative to the observation error in the indent size) is positive for all conditions but is generally larger for the lower applied loads. Notably, although Fig. 7c does not show a significant difference for the residual error in crack length between the 15 s and 30 s dwell time conditions at 0.45 N, less than half of the replicates for these conditions yielded measurable crack patterns (Fig. 3), limiting our ability to draw meaningful conclusions about the reliability of measurements at this low load. For the 30 s dwell time, the residual error decreases with increasing load, and is small for both dwell times at the highest indentation load (1.91 N, Fig. 7a and c). Recall that observation error in indent size is a lower bound estimate for the observation error in crack length, implying that the actual residual error in crack length is smaller than that shown in Fig. 7c, and thus the total error in the crack length measurements may be completely attributable to observation error at 1.91 N; at lower loads, it is likely that other factors contribute to the scatter. The trends in the error in the crack length measurement are mirrored in the residual error in K_c (Fig. 7d). Furthermore, low applied loads and/or short dwell times often lead to errors in the K_c calculations that are not attributable to observation error, as indicated by the large positive values for residual error.

All of these observations suggest that, as with indent size and H_v, utilizing higher applied load and/or longer dwell times improves our ability to accurately determine K_c as a load-independent material property. Returning to Fig. 1, we see that only 60% of previous published work applying the Vickers indentation method to silicate glasses utilizes high load (> 1.06 N) and/or longer dwell times (> 15 s); the remaining *40% of the previously published work utilized the combination of*

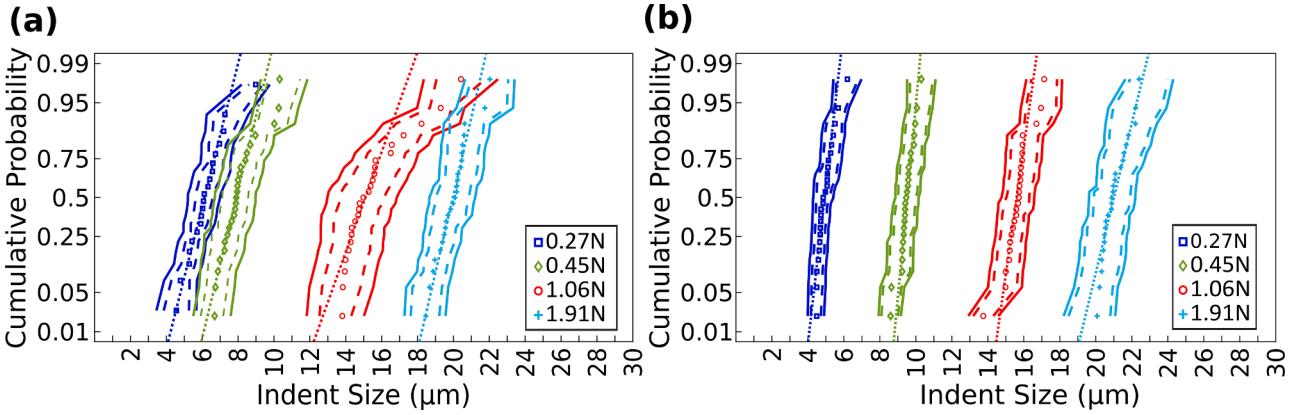

Fig. 6. Cumulative probability plots of indent size as a function of applied load for (a) 15 s and (b) 30 s dwell times, where the y-axis is scaled such that a straight (linear) line corresponds to a normal distribution of the data, as denoted by the dotted lines. The y-axis value represents the probability that a given indent size is less than or equal to the corresponding x-axis value. The dashed and solid boundary lines represent 95% confidence intervals for each individual indent (7 images) and the full data set for a given set of conditions, respectively. The number of data points in each data set is 25 for all conditions except for the 15 s - 0.27 N condition, which includes 20 replicates.

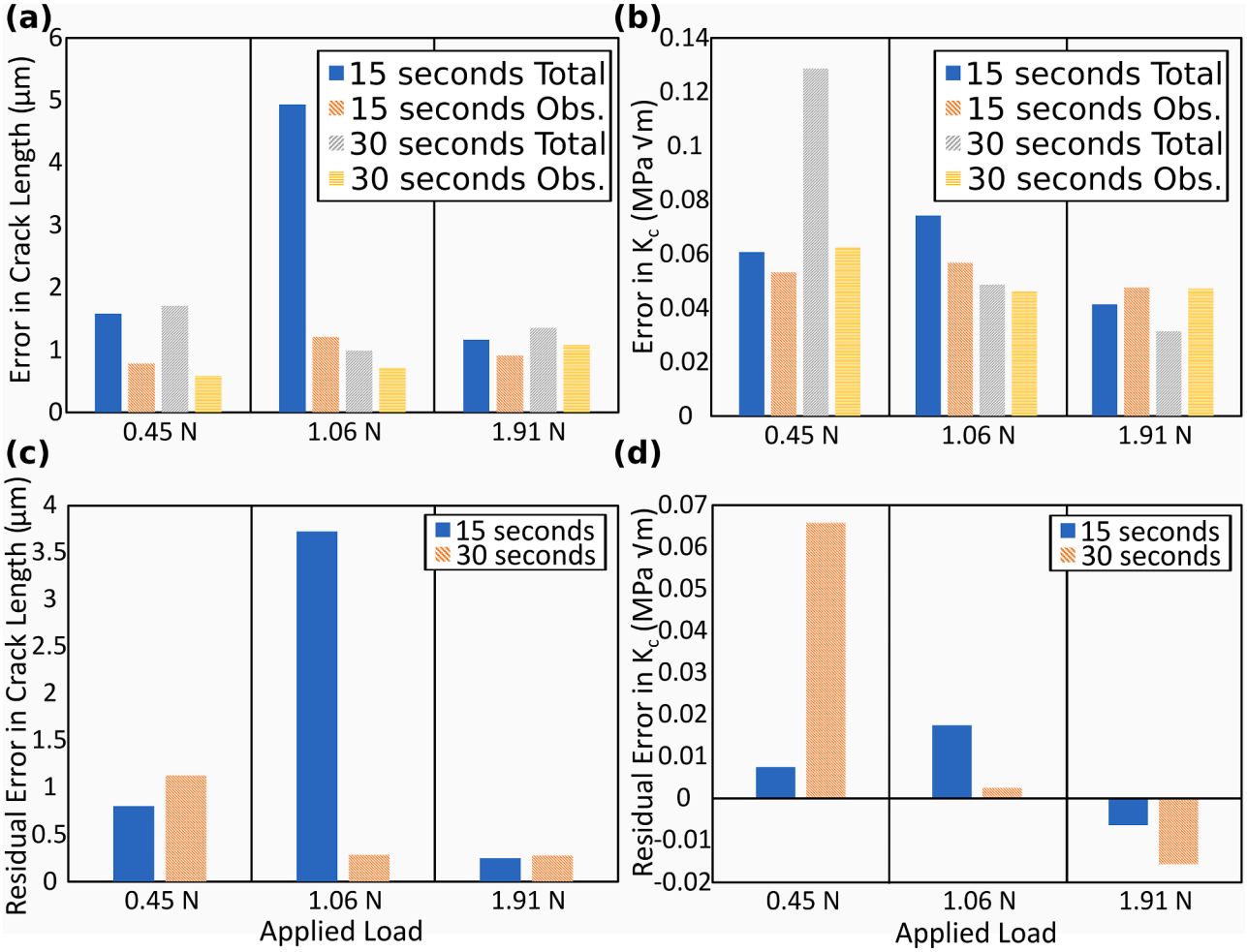

Fig. 7. (a-b): Total and observation errors for (a) crack length and (b) indentation fracture toughness; (c-d): Residual errors in (c) crack length and (d) indentation fracture toughness for various combinations of applied load and dwell time.

low applied load and short dwell time that results in a lack of precision and inconsistencies within the data presented here.

While Vickers indentation has been used in the past to quantify the hardness and indentation fracture toughness of silicate glasses due to the ease of the technique, the inconsistencies associated with measurements within a data set and a lack of reproducibility have limited its utilization for the effective comparison of properties as a function of glass composition or processing conditions. This work suggests that these inconsistencies can be limited by utilizing higher loads and/or longer dwell times, leading to tighter distributions of data and more consistent results, without significantly affecting the total time required to conduct the experiments. Improving the precision and consistency of these measurements would have a significant effect on our ability to accurately measure silicate glass mechanical properties.

5. Conclusion

Here, we have shown that microindentation measurements utilizing a high applied load and/or longer dwell time provide many advantages over traditional low load (< 1.06 N)-short dwell time (≤ 15 s) conditions. Using higher loads and longer dwell time improves the precision of indent size and crack length measurements and leads to a more effective quantification of indentation fracture toughness as a load-independent material property. While this study focuses exclusively on soda-lime glass and investigates a limited number of applied loads and dwell times, the data presented here suggests that the use of higher loads (> 1.06 N) and/or longer dwell time (> 15 s) than is currently standard in the literature may improve the precision of future measurements. While the apparent dependence of these properties on dwell time at low load is interesting from a fundamental perspective, which is beyond the scope of the present study, the fact that precision appears to increase with dwell time could make this technique amenable to the measurement of silicate glass mechanical properties.

Indentation authorship statement

Porter Weeks: Data Curation, Formal Analysis, Investigation, Methodology, Validation Writing-original draft, Writing-review and editing **Katharine Flores:** Funding Acquisition, Project Administration, Supervision, Writing-original draft, Writing-review and editing

The authors declare that the associated manuscript submitted for publication is not published already or under consideration in part or whole in any journal or scientific magazine. We state that all authors listed on the title page have contributed significantly to the work, have read the final version of the manuscript to validate and confirm the content, data and interpretation and agree to its submission in *Journal of Non-Crystalline Solids*.

Declaration of Competing Interest

The authors declare that they have no known competing financial interests or personal relationships that could have appeared to influence the work reported in this paper.

Data availability

Data will be made available on request.

Acknowledgement

This work was supported by the National Science Foundation under Grant No. DMR-2004630.

Supplementary materials

Supplementary material associated with this article can be found, in the online version, at doi:10.1016/j.jnoncrysol.2023.122174.

References

[1] R. Limbach, A. Winterstein-Beckmann, J. Dellith, D. Möncke, L. Wondraczek, Plasticity, crack initiation and defect resistance in alkali-borosilicate glasses: from normal to anomalous behavior, J. Non. Cryst. Solids 417–418 (2015) 15–27, https://doi.org/10.1016/j.jnoncrysol.2015.02.019.
[2] C. Hermansen, J. Matsuoka, S. Yoshida, H. Yamazaki, Y. Kato, Y.Z. Yue, Densification and plastic deformation under microindentation in silicate glasses and the relation to hardness and crack resistance, J. Non. Cryst. Solids 364 (2013) 40–43, https://doi.org/10.1016/j.jnoncrysol.2012.12.047.
[3] A. Pönitzsch, M. Nofz, L. Wondraczek, J. Deubener, Bulk elastic properties, hardness and fatigue of calcium aluminosilicate glasses in the intermediate-silica range, J. Non. Cryst. Solids 434 (2016) 1–12, https://doi.org/10.1016/j.jnoncrysol.2015.12.002.
[4] R.J. Hand, D.R. Tadjiev, Mechanical properties of silicate glasses as a function of composition, J. Non. Cryst. Solids (2010) 2417–2423, https://doi.org/10.1016/j.jnoncrysol.2010.05.007. North-Holland.
[5] E. Kilinc, R.J. Hand, Mechanical properties of soda-lime-silica glasses with varying alkaline earth contents, J. Non. Cryst. Solids 429 (2015) 190–197, https://doi.org/10.1016/j.jnoncrysol.2015.08.013.
[6] R. Limbach, S. Karlsson, G. Scannell, R. Mathew, M. Edén, L. Wondraczek, The effect of TiO2 on the structure of Na2O-CaO-SiO2 glasses and its implications for thermal and mechanical properties, J. Non. Cryst. Solids 471 (2017) 6–18, https://doi.org/10.1016/j.jnoncrysol.2017.04.013.
[7] M. Hojamberdiev, H.J. Stevens, Indentation recovery of soda-lime silicate glasses containing titania, zirconia and hafnia at low temperatures, Mater. Sci. Eng. A 532 (2012) 456–461, https://doi.org/10.1016/j.msea.2011.11.012.
[8] N. Kedir, D.C. Faucett, S.R. Choi, N.P. Bansal, Slow-crack-growth and indentation damage in calcium magnesium aluminosilicate (CMAS) glass from desert sand, Ceram. Int. 44 (2018) 2676–2682, https://doi.org/10.1016/j.ceramint.2017.10.194.
[9] S. Dériano, A. Jarry, T. Rouxel, J.C. Sangleboeuf, S. Hampshire, The indentation fracture toughness (kc) and its parameters: the case of silica-rich glasses, J. Non. Cryst. Solids (2004) 44–50, https://doi.org/10.1016/j.jnoncrysol.2004.07.021.
[10] M. Barlet, J.M. Delaye, T. Charpentier, M. Gennisson, D. Bonamy, T. Rouxel, C. L. Rountree, Hardness and toughness of sodium borosilicate glasses via Vickers's indentations, J. Non. Cryst. Solids 417–418 (2015) 66–79, https://doi.org/10.1016/j.jnoncrysol.2015.02.005.
[11] S. Kasimuthumaniyan, A.A. Reddy, N.M.A. Krishnan, N.N. Gosvami, Understanding the role of post-indentation recovery on the hardness of glasses: case of silica, borate, and borosilicate glasses, J. Non. Cryst. Solids 534 (2020), 119955, https://doi.org/10.1016/J.JNONCRYSOL.2020.119955.
[12] S. Yoshida, J.C. Sanglebœuf, T. Rouxel, Quantitative evaluation of indentation-induced densification in glass, J. Mater. Res. 20 (2005) 3404–3412, https://doi.org/10.1557/jmr.2005.0418.
[13] G.N.B.M. de Macedo, S. Sawamura, L. Wondraczek, Lateral hardness and the scratch resistance of glasses in the Na2O-CaO-SiO2 system, J. Non. Cryst. Solids 492 (2018) 94–101, https://doi.org/10.1016/j.jnoncrysol.2018.04.022.
[14] H. Morozumi, S. Yoshida, J. Matsuoka, Composition dependence of crack formation probability in aluminoborosilicate glass, J. Non. Cryst. Solids 444 (2016) 31–37, https://doi.org/10.1016/j.jnoncrysol.2016.04.030.
[15] J. Kjeldsen, M.M. Smedskjaer, J.C. Mauro, Y. Yue, On the origin of the mixed alkali effect on indentation in silicate glasses, J. Non. Cryst. Solids 406 (2014) 22–26, https://doi.org/10.1016/j.jnoncrysol.2014.09.036.
[16] M.M. Smedskjaer, M. Jensen, Y. Yue, Effect of thermal history and chemical composition on hardness of silicate glasses, J. Non. Cryst. Solids 356 (2010) 893–897, https://doi.org/10.1016/j.jnoncrysol.2009.12.030.
[17] J. Sehgal, S. Ito, Brittleness of glass, J. Non. Cryst. Solids 253 (1999) 126–132, https://doi.org/10.1016/S0022-3093(99)00348-8.
[18] P. Sellappan, T. Rouxel, F. Celarie, E. Becker, P. Houizot, R. Conradt, Composition dependence of indentation deformation and indentation cracking in glass, Acta Mater 61 (2013) 5949–5965, https://doi.org/10.1016/j.actamat.2013.06.034.
[19] M. Tiegel, R. Hosseinabadi, S. Kuhn, A. Herrmann, C. Rüssel, Young's modulus, Vickers hardness and indentation fracture toughness of alumino silicate glasses, Ceram. Int. 41 (2015) 7267–7275, https://doi.org/10.1016/j.ceramint.2015.01.144.
[20] I. Hasdemir, S. Striepe, J. Deubener, K. Simon, A 2000-year perspective on indentation crack resistance and brittleness of glass, J. Non. Cryst. Solids 408 (2015) 51–56, https://doi.org/10.1016/j.jnoncrysol.2014.10.012.
[21] T.K. Bechgaard, A. Goel, R.E. Youngman, J.C. Mauro, S.J. Rzoska, M. Bockowski, L. R. Jensen, M.M. Smedskjaer, Structure and mechanical properties of compressed sodium aluminosilicate glasses: role of non-bridging oxygens, J. Non. Cryst. Solids 441 (2016) 49–57, https://doi.org/10.1016/j.jnoncrysol.2016.03.011.
[22] K. Januchta, R.E. Youngman, A. Goel, M. Bauchy, S.J. Rzoska, M. Bockowski, M. M. Smedskjaer, Structural origin of high crack resistance in sodium aluminoborate glasses, J. Non. Cryst. Solids 460 (2017) 54–65, https://doi.org/10.1016/j.jnoncrysol.2017.01.019.
[23] S. Yoshida, A. Hidaka, J. Matsuoka, Crack initiation behavior of sodium aluminosilicate glasses, J. Non. Cryst. Solids (2004) 37–43, https://doi.org/10.1016/j.jnoncrysol.2004.07.019. North-Holland.
[24] Y. Hayashi, Y. Fukuda, M. Kudo, Investigation on changes in surface composition of float glass - mechanisms and effects on the mechanical properties, Surf. Sci. (2002) 872–876, https://doi.org/10.1016/S0039-6028(02)01365-1. North-Holland.
[25] T.K. Bechgaard, J.C. Mauro, M.M. Smedskjaer, Time and humidity dependence of indentation cracking in aluminosilicate glasses, J. Non. Cryst. Solids 491 (2018) 64–70, https://doi.org/10.1016/j.jnoncrysol.2018.04.009.
[26] K. Januchta, R.E. Youngman, A. Goel, M. Bauchy, S.L. Logunov, S.J. Rzoska, M. Bockowski, L.R. Jensen, M.M. Smedskjaer, Discovery of ultra-crack-resistant oxide glasses with adaptive networks, Chem. Mater. 29 (2017) 5865–5876, https://doi.org/10.1021/acs.chemmater.7b00921.
[27] S. Kapoor, N. Lönnroth, R.E. Youngman, S.J. Rzoska, M. Bockowski, L.R. Jensen, M.M. Smedskjaer, Pressure-driven structural depolymerization of zinc phosphate glass, J. Non. Cryst. Solids 469 (2017) 31–38, https://doi.org/10.1016/j.jnoncrysol.2017.04.011.
[28] S. Kapoor, X. Guo, R.E. Youngman, C.L. Hogue, J.C. Mauro, S.J. Rzoska, M. Bockowski, L.R. Jensen, M.M. Smedskjaer, Network Glasses under Pressure: permanent Densification in Modifier-Free Al2 O3- B2 O3- P2 O5-SiO2 Systems, Phys. Rev. Appl. 7 (2017), 054011, https://doi.org/10.1103/PhysRevApplied.7.054011.
[29] G.A. Rosales-Sosa, A. Masuno, Y. Higo, H. Inoue, Y. Yanaba, T. Mizoguchi, T. Umada, K. Okamura, K. Kato, Y. Watanabe, High elastic moduli of a 54Al2O3-46Ta2O5 glass fabricated via containerless processing, Sci. Rep. 5 (2015) 1–8, https://doi.org/10.1038/srep15233.
[30] T. Toninato, R. Dall'igna, V. Gottardi, R. Dal Maschio, S. Gatta, G. Scarinci, Crack nucleation in ultrathin blown silicate glasses, J. Non. Cryst. Solids 80 (1986) 481–486, https://doi.org/10.1016/0022-3093(86)90435-7.
[31] H. Morozumi, H. Nakano, S. Yoshida, J. Matsuoka, Crack initiation tendency of chemically strengthened glasses, Int. J. Appl. Glas. Sci. 6 (2015) 64–71, https://doi.org/10.1111/ijag.12089.
[32] G.A. Rosales-Sosa, A. Masuno, Y. Higo, H. Inoue, Crack-resistant Al2O3-SiO2 glasses, Sci. Rep. 6 (2016) 1–7, https://doi.org/10.1038/srep23620.
[33] A. Talimian, V.M. Sglavo, Can annealing improve the chemical strengthening of thin borosilicate glass? J. Non. Cryst. Solids 465 (2017) 1–7, https://doi.org/10.1016/j.jnoncrysol.2017.03.038.
[34] Y. Kato, H. Yamazaki, S. Yoshida, J. Matsuoka, Effect of densification on crack initiation under Vickers indentation test, J. Non. Cryst. Solids 356 (2010) 1768–1773, https://doi.org/10.1016/j.jnoncrysol.2010.07.015.
[35] S. Yoshida, Y. Nishikubo, A. Konno, T. Sugawara, Y. Miura, J. Matsuoka, Fracture- and indentation-induced structural changes of sodium borosilicate glasses, Int. J. Appl. Glas. Sci. 3 (2012) 3–13, https://doi.org/10.1111/j.2041-1294.2011.00077.x.
[36] K.G. Aakermann, K. Januchta, J.A.L. Pedersen, M.N. Svenson, S.J. Rzoska, M. Bockowski, J.C. Mauro, M. Guerette, L. Huang, M.M. Smedskjaer, Indentation deformation mechanism of isostatically compressed mixed alkali aluminosilicate glasses, J. Non. Cryst. Solids 426 (2015) 175–183, https://doi.org/10.1016/j.jnoncrysol.2015.06.028.
[37] S. Striepe, M. Potuzak, M.M. Smedskjaer, J. Deubener, Relaxation kinetics of the mechanical properties of an aluminosilicate glass, J. Non. Cryst. Solids 362 (2013) 40–46, https://doi.org/10.1016/j.jnoncrysol.2012.11.017.
[38] M.N. Svenson, T.K. Bechgaard, S.D. Fuglsang, R.H. Pedersen, A.O. Tjell, M. B. Østergaard, R.E. Youngman, J.C. Mauro, S.J. Rzoska, M. Bockowski, M. M. Smedskjaer, Composition-structure-property relations of compressed borosilicate glasses, Phys. Rev. Appl. 2 (2014), 024006, https://doi.org/10.1103/PhysRevApplied.2.024006.
[39] M. Barlet, A. Kerrache, J.M. Delaye, C.L. Rountree, SiO2-Na2O-B2O3 density: a comparison of experiments, simulations, and theory, J. Non. Cryst. Solids 382 (2013) 32–44, https://doi.org/10.1016/j.jnoncrysol.2013.09.022.
[40] S. Inaba, S. Fujino, K. Morinaga, Young's modulus and compositional parameters of oxide glasses, J. Am. Ceram. Soc. 82 (2004) 3501–3507, https://doi.org/10.1111/j.1151-2916.1999.tb02272.x.
[41] A. Pedone, G. Malavasi, M. Cristina Menziani, U. Segre, A.N. Cormack, Role of magnesium in soda-lime glasses: insight into structural, transport, and mechanical properties through computer simulations, J. Phys. Chem. C 112 (2008) 11034–11041, https://doi.org/10.1021/jp8016776.
[42] M. Ren, J.Y. Cheng, S.P. Jaccani, S. Kapoor, R.E. Youngman, L. Huang, J. Du, A. Goel, Composition – structure – property relationships in alkali aluminosilicate glasses: a combined experimental – computational approach towards designing functional glasses, J. Non. Cryst. Solids 505 (2019) 144–153, https://doi.org/10.1016/j.jnoncrysol.2018.10.053.
[43] C. Zehnder, S. Bruns, J.-.N. Peltzer, K. Durst, S. Korte-Kerzel, D. Möncke, Influence of cooling rate on cracking and plastic deformation during impact and indentation

of borosilicate glasses, Front. Mater. 4 (2017) 5, https://doi.org/10.3389/fmats.2017.00005.
[44] Q. Zhao, M. Guerette, L. Huang, Nanoindentation and Brillouin light scattering studies of elastic moduli of sodium silicate glasses, J. Non. Cryst. Solids 358 (2012) 652–657, https://doi.org/10.1016/j.jnoncrysol.2011.10.034.
[45] O. Goodman, B. Derby, The mechanical properties of float glass surfaces measured by nanoindentation and acoustic microscopy, Acta Mater. 59 (2011) 1790–1799, https://doi.org/10.1016/j.actamat.2010.11.045.
[46] M. Barlet, J.M. Delaye, B. Boizot, D. Bonamy, R. Caraballo, S. Peuget, C. L. Rountree, From network depolymerization to stress corrosion cracking in sodium-borosilicate glasses: effect of the chemical composition, J. Non. Cryst. Solids 450 (2016) 174–184, https://doi.org/10.1016/j.jnoncrysol.2016.07.017.
[47] S.M. Wiederhorn, Influence of water vapor on crack propagation in soda-lime glass, J. Am. Ceram. Soc. 50 (1967) 407–414, https://doi.org/10.1111/j.1151-2916.1967.tb15145.x.
[48] S.M. Wiederhorn, L.H. Bolz, Stress corrosion and static fatigue of glass, J. Am. Ceram. Soc. 53 (1970) 543–548, https://doi.org/10.1111/j.1151-2916.1970.tb15962.x.
[49] S.W. Freiman, S.M. Wiederhorn, J.J. Mecholsky, Environmentally enhanced fracture of glass: a historical perspective, J. Am. Ceram. Soc. (2009) 1371–1382, https://doi.org/10.1111/j.1551-2916.2009.03097.x. John Wiley & Sons, Ltd.
[50] R. Gy, Stress corrosion of silicate glass: a review, J. Non. Cryst. Solids (2003) 1–11, https://doi.org/10.1016/S0022-3093(02)01931-2. North-Holland.
[51] M. Ciccotti, Stress-corrosion mechanisms in silicate glasses, J. Phys. D Appl. Phys. 42 (2009).
[52] Y. Kato, H. Yamazaki, S. Itakura, S. Yoshida, J. Matsuoka, Load dependence of densification in glass during Vickers indentation test, J. Ceram. Soc. Jpn. 119 (2011) 110–115, https://doi.org/10.2109/jcersj2.119.110.
[53] T.M. Gross, M. Tomozawa, Crack-free high load Vickers indentation of silica glass, J. Non. Cryst. Solids 354 (2008) 5567–5569, https://doi.org/10.1016/j.jnoncrysol.2008.09.015.
[54] T.M. Gross, Deformation and cracking behavior of glasses indented with diamond tips of various sharpness, J. Non. Cryst. Solids (2012) 3445–3452, https://doi.org/10.1016/j.jnoncrysol.2012.01.052. North-Holland.
[55] J. Suwanprateeb, A comparison of different methods in determining load- and time-dependence of Vickers hardness in polymers, Polym. Test. 17 (1998) 495–506, https://doi.org/10.1016/S0142-9418(97)00040-8.
[56] O. Yoldas, T. Akova, H. Uysal, Influence of different indentation load and dwell time on Knoop microhardness tests for composite materials, Polym. Test. 23 (2004) 343–346, https://doi.org/10.1016/S0142-9418(03)00104-1.
[57] K. Hirao, M. Tomozawa, Microhardness of SiO2 glass in various environments, J. Am. Ceram. Soc. 70 (1987) 497–502, https://doi.org/10.1111/j.1151-2916.1987.tb05683.x.
[58] Y. Song, Y. Ma, Z. Pan, Y. Li, T. Zhang, Z. Gao, Nanoindentation characterization of creep-fatigue interaction on local creep behavior of P92 steel welded joint, Chin. J. Mech. Eng. 34 (2021) 131, https://doi.org/10.1186/s10033-021-00661-5.
[59] R.A. Tarefder, H. Faisal, Effects of dwell time and loading rate on the nanoindentation behavior of asphaltic materials, J. Nanomech. Micromech. 3 (2013) 17–23, https://doi.org/10.1061/(ASCE)NM.2153-5477.0000054.
[60] B.R. Lawn, T.P. Dabbs, C.J. Fairbanks, Kinetics of shear-activated indentation crack initiation in soda-lime glass, J. Mater. Sci. 18 (1983) 2785–2797, https://doi.org/10.1007/BF00547596.
[61] A. International, Standard Test Method For Knoop and Vickers Hardness of Materials, ASTM Stand, 2011.
[62] H. Li, R.C. Bradt, The indentation load/size effect and the measurement of the hardness of vitreous silica, J. Non. Cryst. Solids 146 (1992) 197–212, https://doi.org/10.1016/S0022-3093(05)80492-2.
[63] M. Kazembeyki, M. Bauchy, C.G. Hoover, New insights into the indentation size effect in silicate glasses, J. Non. Cryst. Solids 521 (2019), 119494, https://doi.org/10.1016/J.JNONCRYSOL.2019.119494.
[64] M.M. Smedskjaer, Indentation size effect and the plastic compressibility of glass, Appl. Phys. Lett. 104 (2014), 251906, https://doi.org/10.1063/1.4885337.
[65] H. Li, A. Ghosh, Y.H. Han, R.C. Bradt, The frictional component of the indentation size effect in low load microhardness testing, J. Mater. Res. 1993 85 (8) (2011) 1028–1032, https://doi.org/10.1557/JMR.1993.1028.
[66] W.D. Nix, H. Gao, Indentation size effects in crystalline materials: a law for strain gradient plasticity, J. Mech. Phys. Solids 46 (1998) 411–425, https://doi.org/10.1016/S0022-5096(97)00086-0.
[67] T. Rouxel, Driving force for indentation cracking in glass: composition, pressure and temperature dependence, Philos. Trans. R. Soc. A Math. Phys. Eng. Sci. 373 (2015), https://doi.org/10.1098/RSTA.2014.0140.
[68] M. Liu, D. Hou, Y. Wang, G. Lakshminarayana, Micromechanical properties of Dy3 + ion-doped (Lu Y1-)3Al5O12 (x = 0, 1/3, 1/2) single crystals by indentation and scratch tests, Ceram. Int. (2022), https://doi.org/10.1016/j.ceramint.2022.09.334.
[69] M. Liu, Z. Xu, R. Fu, Micromechanical and microstructure characterization of BaO-Sm2O3–5TiO2 ceramic with addition of Al2O3, Ceram. Int. 48 (2022) 992–1005, https://doi.org/10.1016/j.ceramint.2021.09.184.
[70] C.A. Schneider, W.S. Rasband, K.W. Eliceiri, NIH Image to ImageJ: 25 years of image analysis, Nat. Methods 9 (2012) 671–675, https://doi.org/10.1038/nmeth.2089.
[71] G.R. Anstis, P. Chantikul, B.R. Lawn, D.B. Marshall, A critical evaluation of indentation techniques for measuring fracture toughness: I, direct crack measurements, J. Am. Ceram. Soc. 64 (1981) 533–538, https://doi.org/10.1111/j.1151-2916.1981.tb10320.x.
[72] All about soda-lime glass: composition and properties, (n.d.) (2023). https://www.thomasnet.com/articles/plant-facility-equipment/soda-lime-glass/.
[73] K. Niihara, R. Morena, D.P.H. Hasselman, Evaluation ofK Ic of brittle solids by the indentation method with low crack-to-indent ratios, J. Mater. Sci. Lett. 1 (1982) 13–16, https://doi.org/10.1007/BF00724706.
[74] E.R. Cohen, An introduction to error analysis: the study of uncertainties in physical measurements, Meas. Sci. Technol. 9 (1998), https://doi.org/10.1088/0957-0233/9/6/022.